ELSEVIER

Chemical Engineering Journal 74 (1999) 147–153

Chemical Engineering Journal

Fully developed turbulent flow in ducts with symmetric and asymmetric rough walls

L.C.G. Pimentel[a,*], R.M. Cotta[1,a], S. Kakaç[b]

[a]*Laboratory of Transmission and Technology of Heat - LTTC, PEM/COPPE-DEM/EE, Universidade Federal do Rio de Janeiro, Cx Postal 68503, Rio de Janeiro 21945-970, Brazil*

[b]*Mechanical Engineering Department, College of Engineering, University of Miami, Coral Gables, FL 33124, USA*

Received 5 May 1998; received in revised form 1 December 1998; accepted 10 January 1999

Abstract

A low computational cost semi-analytical procedure is presented for the solution of incompressible fully developed turbulent flow through symmetric and asymmetric ducts with rough walls. Using a modified algebraic turbulence model to represent the influence of rough surfaces, the flow field in ducts with different wall roughnesses is solved. The velocity distribution and the friction factor in two different geometries, circular duct and parallel plates, are presented and compared with experimental and numerical data available in the literature, and a satisfactory agreement is obtained.

Keywords: Turbulent flow; Symmetric; Asymmetric; Rough walls

1. Introduction

Turbulent flow over rough surfaces has been a subject of increasing interest in the areas of heat transfer and fluid dynamics over the last few years. Flows of this nature can be found in engineering systems of significant technological interest such as turbine blade internal cooling, advanced gas-cooled nuclear reactor, heat exchangers and cooling of microelectronic devices. Other examples of great relevance have been pointed out by McEligot and McEligot [1].

An early systematic investigation of the effects of Reynolds number and relative roughness on friction factor and velocity distribution in pipe flow was performed by Nikuradse [2]. His work showed that the relation between the resistance formula and velocity distribution within smooth pipes could be extended to the case of rough pipes [3].

Several experimental works have been performed to provide information about pressure drop [4], velocity distribution and turbulent flow structure near rough walls [5–7], and heat transfer as a function of the ratio of roughness height to hydraulic diameter, spacing between roughness elements and Reynolds number [8–10]. Wassel and Mills [11] and Youn et al. [12] related the first two magnitudes, rib height and rib pitch, to an equivalent sand roughness as studied by Nikuradse [2].

Powe and Townes [13] investigated the turbulence structure for fully developed flow in rough pipes. The method used to determine the turbulence structure was an examination of the fluctuating velocity spectra in all three coordinate directions. An important conclusion of this work was that in the central region of the pipe, the flow is relatively independent of the nature of the solid boundary. In contrast, the flow near the wall presents a marked dependence on the nature of the solid boundary.

A few different ways of representing the effects of rough surfaces on turbulent flows have been proposed previously. Wassel and Mills [11] dealt with the turbulent flow in ducts with rough walls by using a mixing-length model in the turbulent core and a roughness element drag coefficient to characterize transport at the wall region. Webb et al. [14], in their experimental study about tubes with repeated-rib roughness, developed a friction factor correlation based on the law of the wall similarity. In a recent work, Koh [15] presented a formula to represent the mean-velocity distribution across the inner layer of a turbulent boundary layer and used this velocity profile to derive a friction factor correlation for a fully developed turbulent pipe flow. A more advanced analysis was performed by Youn et al. [12] viz. the so-called wall-function approach where the transport equation and the turbulence model are solved only beyond a

*Corresponding author.

[1]E-mail: cotta@serv.com.ufrj.br

1385-8947/99/$ – see front matter
PII: S1385-8947(99)00036-4

specified position away from the wall and all the boundary conditions are specified at this location. In their numerical simulation of incompressible turbulent flow in a rectangular duct with one side rib-roughened, Youn et al. [12] employed a k–ε turbulence model with an empirical wall function to capture the effects of the rough surface. Other important works with the k–ε turbulence model were conducted by Liou et al. [16] and Tarada [17]. Another approach was presented by Hatton and Walklate [18], Feiereisen and Acharya [19], Vulchanov and Zimparov [20] and Han [21], wherein using a modified mixing-length model to represent the influence of the rough wall, they solved the flow field in internal and external flows. Although it cannot consider the flow between the roughness elements, this approach presents advantages as regards computational cost reduction as compared to the k–ε model approach. Besides, it can be used within a reasonable degree of accuracy for walls with moderate roughness.

A classical numerical approach to turbulent flow over rough surfaces was proposed by Cebeci and Chang [22]. By using the algebraic eddy viscosity of Cebeci and Chang [23], and incorporating a suggestion by Rotta (in [22]) to represent the influence of the rough surface on the flow near the wall, they dealt with the incompressible rough wall boundary layer flow. The applicability of the procedure, confirmed by the comparison of calculated and measured values of the skin friction available in the literature, brought about the use of similar approaches to solve the fully developed internal flow in ducts with symmetric and asymmetric rough walls.

In this work, a semi-analytical procedure is developed and results are presented for friction factor and velocity distribution in two different geometries, parallel plate channels and circular ducts, for three different flow regimes (hydraulically smooth, transitional and fully rough). The present approach is aimed especially at providing an analytical solution to internal flows in parallel-plate channels with moderate sand grain roughness on the two opposite sides, which shall be particularly useful in heat transfer simulations and in the analysis to follow.

2. Problem formulation

We consider incompressible fully developed turbulent flow of a Newtonian fluid through ducts with rough walls, subjected to non-slip condition on the walls. In the case of circular ducts, the additional symmetry condition in the centerline is considered. The eddy viscosity concept is considered to be adequate and all the dependent variables are time-averaged quantities. Under these assumptions, the continuity and the momentum transport equations can be written in dimensionless form as

Continuity:

$$\frac{\mathrm{d}(U_{\mathrm{FD}})}{\mathrm{d}x} = 0 \tag{1}$$

Momentum:

$$\frac{1}{r^k}\frac{\mathrm{d}}{\mathrm{d}r}\left[r^k(1+\varepsilon_{\mathrm{FD}})\frac{\mathrm{d}}{\mathrm{d}r}(U_{\mathrm{FD}})\right] - \mathrm{Re}\,\frac{\mathrm{d}P}{\mathrm{d}x} = 0 \tag{2}$$

Boundary conditions:

$$U_{\mathrm{FD}} = 0 \quad \text{at} \quad r = b$$

$$(1-k)U_{\mathrm{FD}} + k\frac{\mathrm{d}(U_{\mathrm{FD}})}{\mathrm{d}r} = 0 \quad \text{at} \quad r = 0 \tag{3}$$

and

$$k = \begin{cases} 0 & \text{Parallel plates} \\ 1 & \text{Circular duct} \end{cases}$$

The various dimensionless groups are defined as

$$r = \frac{\bar{r}}{b}; \quad x = \frac{\bar{x}}{b}; \quad U_{\mathrm{FD}} = \frac{u_{\mathrm{FD}}}{U_0}; \quad P = \frac{\bar{P} + \rho g S x}{\rho U_0^2};$$

$$\mathrm{Re} = \frac{U_0 b}{\nu}; \quad \varepsilon_{\mathrm{FD}} = \frac{\nu_\tau}{\nu}$$

The modified pressure field, P, allows for the simulation of inclined channels.

By using an appropriate coordinate system, the turbulence model proposed by Cebeci and Chang [22] can be written for two distinct regions. The first one goes from the bottom wall to the position where the velocity is maximum ($r = r_{\mathrm{m}}$) and the second region goes from the position $r = r_{\mathrm{m}}$ to the top wall, where $\varepsilon_{\mathrm{FD}i}$ is given for instance (parallel plates), by

$$\varepsilon_{\mathrm{FD}} = \frac{\mathrm{Re}}{4}L_i^2(r)\left\{1 - \exp\left(\frac{\left((-1)^{1-i}2r - 2(i)\right)}{26}\sqrt{\frac{\mathrm{Re}}{4}(1+\varepsilon_{\mathrm{FD}i})\left.\frac{\mathrm{d}(U_{\mathrm{FD}})}{\mathrm{d}y}\right|_{r=i}} - \frac{\Delta r_i}{A}\right)\right\}^2 \left|\frac{\mathrm{d}(U_{\mathrm{FD}})}{\mathrm{d}r}\right| \tag{4}$$

where the dimensionless modified Nikuradse mixing-length, presented by Cebeci and Chang [23] and incorporating the suggestion by Rotta (in [22]) to represent the influence of the rough surface in the flow near the wall can be written as

$$L_i(r) = 0.14 - 0.08\left(-2r + 1 - \left(\frac{2^{1-k}\,\Delta r_i}{b}\right)\right)^2 - 0.06\left(-2r + 1 - \left(\frac{2^{1-k}\,\Delta r_i}{b}\right)\right)^4 \tag{5}$$

where

$$A = \frac{26\nu}{u_\tau}$$

The dimensionless shift coordinate, $\Delta r_i/b$, is given by

$$\frac{\Delta r_i}{b} = 0, \quad 0 < K_{s_i}^+ < 5 \tag{6a}$$

$$\frac{\Delta r_i}{b} = \frac{0.9K_{s_i}}{b}\left[\sqrt{\frac{1}{K_{s_i}^+}} - \exp\left(-\frac{K_{s_i}^+}{6}\right)\right], \quad 5 \le K_{s_i}^+ < 70 \tag{6b}$$

$$\frac{\Delta r_i}{b} = \frac{0.7K_{s_i}}{b}\frac{1}{K_{s_i}^+}\left[(K_s^+)^{0,58}\right], \quad K_{s_i}^+ \ge 70 \tag{6c}$$

and the dimensionless shift coordinate, $\Delta r_i/A$, becomes

$$\frac{\Delta r_i}{A} = 0, \quad 0 < K_{s_i}^+ < 5 \tag{7a}$$

$$\frac{\Delta r_i}{A} = \frac{0.9}{26}\left[\sqrt{K_{s_i}^+} - K_{s_i}^+ \exp\left(-\frac{K_{s_i}^+}{6}\right)\right], \quad 5 \le K_{s_i}^+ < 70 \tag{7b}$$

$$\frac{\Delta r_i}{A} = \frac{0.7}{26}\left[(K_s^+)^{0,58}\right], \quad K_{s_i}^+ \ge 70 \tag{7c}$$

where the equivalent sand grain roughness parameter, $K_{s_i}^+$, is written as a function of the Reynolds number and the relative roughness as

$$K_{s_i}^+ = \frac{K_{s_i}}{b}\sqrt{(-1)^i \mathrm{Re}(1+\varepsilon_{\mathrm{FD}i})\left.\frac{\mathrm{d}(U_{\mathrm{FD}})}{\mathrm{d}r}\right|_{r=i}};$$

$$\text{and } i = \begin{cases} 0, & \text{Bottom wall} \\ 1, & \text{Top wall} \end{cases} \tag{8}$$

The relative roughness, k_s/b, can be replaced with the aid of geometric parameters like the rib height and the pitch between them, following the correlation introduced by Youn et al. [12] to simulate ribbed channels:

$$\frac{K_s}{b} = \frac{h_{\mathrm{rib}}}{b}\exp\left[k(8.5 - u_h^+)\right]; \quad \text{where } k = 0.41 \tag{9a}$$

and

$$u_h^+ = \left(1 - \frac{h_{\mathrm{rib}}}{b}\right)\left(\frac{\mathrm{pitch}}{h_{\mathrm{rib}}}\right)^{0.5} \tag{9b}$$

In this work, we follow the hypothesis that the zero Reynolds stress and the maximum velocity planes are coincident at $r = r_m$. However, a study by Hanjalic and Launder [24] on fully developed flow goes against this hypothesis. In that experimental work, the asymmetry was introduced by roughness on one side of the channel, while the other side was left smooth, and the ratio between the shear stresses on the two surfaces was 4 : 1. In a recent work, Parthasaraty and Muste [25] confirmed the non-coincidence of the planes of maximum velocity and zero Reynolds stress. However, in their study, the shear stress at the bottom and the top surfaces was of the same order of magnitude and the difference between the positions of the two planes was small. Hence, here, the simulation of asymmetric flows is not believed to be highly dependent on this assumption.

Following this consideration, the velocity profile within the regions I and II can be found by integrating Eq. (2) between r and r_m, and by using the boundary condition at $r = 0$, and between r_m and r, as well as the boundary condition at $r = 1$, respectively. Then, defining $C = \mathrm{Re}(\mathrm{d}P/\mathrm{d}x)$, one finds for each region

$$\frac{\mathrm{d}(U_{\mathrm{FD}_i})}{\mathrm{d}r} = -\frac{\left(2^{1-k}\right)C(r_m - r)}{\left(1 + \sqrt{\left(1 - (2^{k+1})G_i(r)C\left((-1)^i(r_m - r)\right)\right)}\right)} \tag{10}$$

The velocity distribution in each region can be obtained by direct integration of Eq. (10).

3. Non-linear algebraic system

A system of non-linear algebraic equations can be organized to determine the variables

$$C, \quad \left.\frac{\mathrm{d}(U_{\mathrm{FD}})}{\mathrm{d}r}\right|_{r=0}, \quad \left.\frac{\mathrm{d}(U_{\mathrm{FD}})}{\mathrm{d}r}\right|_{r=1}, \quad K_{s_0}^+, \quad K_{s_1}^+, \quad r_m$$

The required six algebraic equations are given by Eqs. (8) and (10) applied in $r = 0$ and $r = 1$, in conjunction with the mass conservation equation

$$2^k \int_0^{r_m} r^k U_{\mathrm{FD}_0}\,\mathrm{d}r + 2^k \int_{r_m}^1 r^k U_{\mathrm{FD}_1}\,\mathrm{d}r = 2^k \tag{11}$$

and the matching of the velocity profile

$$U_{\mathrm{FD}_0}(r_m) = U_{\mathrm{FD}_1}(r_m) \tag{12}$$

The non-linear system is solved with subroutine DNEQNF from the IMSL library [26], that solves a system of non-linear equations using a modified Powell hybrid algorithm and a finite-difference approximation to the Jacobian. The stopping criterion, an input in the algorithm, considers the root as accepted if the relative error between two successive approximations to this root is less than an user prescribed accuracy, and in our procedure, we use a tolerance equal to 10^{-11}. During the process, it is necessary to solve a double integral in order to find the velocity profile and mass conservation Eq. (11), and we use subroutine DTWODQ from the ISML library [26] within a relative tolerance equal to 10^{-11} that does not allow for error propagation in the non-linear system solution.

4. Results and discussion

4.1. Symmetric flow

The calculation of friction factor in rough tubes is illustrated in Table 1. The values of f were calculated with two

Table 1
Results of Fanning friction factor in rough tubes at different flow regimes

Case	$K_s/D \times 10^2$	K_s^+	$Re_D \times 10^{-4}$	Nikuradse [2]	Vulchanov and Zimparov [20]	This work[a]	This work[b]
				$(f \times 10^2)$	$(f \times 10^2)$	$(f \times 10^2)$	$(f \times 10^2)$
1	1.634	22.6	1.95	1.037	1.030	0.947	1.010
2		74.9	6.30	1.109	1.060	0.987	1.061
3		222.5	17.99	1.122	1.085	1.001	1.146
4		786.6	64.60	1.140	1.027	0.962	1.100
5	0.833	34.3	6.50	0.843	0.835	0.781	0.805
6		57.8	10.79	0.867	0.841	0.798	0.829
7		223.1	39.80	0.887	0.863	0.810	0.906
8		345.6	61.50	0.889	0.857	0.806	0.907
9		510.0	91.60	0.897	0.843	0.794	0.896
10	0.397	15.0	6.60	0.632	0.625	0.600	0.658
11		40.3	17.80	0.682	0.669	0.632	0.650
12		148.3	62.80	0.705	0.685	0.647	0.708
13		230.9	97.05	0.700	0.687	0.650	0.719
14	0.198	7.1	6.10	0.532	0.524	0.500	0.588
15		10.2	9.71	0.552	0.510	0.485	0.563
16		19.7	19.20	0.537	0.532	0.504	0.537
17		63.7	61.20	0.581	0.556	0.528	0.553

[a] Relation for transitional flow regime Eqs. (6b) and (7b).
[b] Relation for fully rough flow regime Eqs. (6c) and (7c).

different relations for Δr, as presented by Cebeci and Bradshaw [27]. The first one was proposed for transitional regime ($5 < K_s^+ < 70$), Eqs. (6b) and (7b) of the present work, while the second was recommended for fully rough flow Eqs. (6c) and (7c). However, in the present work, each one was used in all the flow regimes, as shown in Table 1, in order to establish the real range of application. It should be noted that Eqs. (9a) and (9b) were not employed in the results obtained for Table 1 since the values of K_s^+ considered were those directly extracted from the values of K_s and D in [20].

The comparison of calculated friction factor with experimental data given by Nikuradse [2] shows that the use of Eqs. (6c) and (7c) in the numerical procedure presents differences less than 5%, excluding case 14 (10%). In fully rough flow regime, this difference is less than 3%, while the use of Eqs. (6b) and (7b) presents a worse agreement of calculated friction factor in all the flow regimes, the percent difference with respect to Nikuradse's data [2] being less than 9% in the transitional regime and less than 12% in the fully rough regime.

Fig. 1 presents a comparison of the universal velocity profile in circular duct flow with empirical correlations [3] for fully rough, transitional and hydraulically smooth flow regimes. The results show that the present numerical procedure offers good agreement with the experimental results for all the flow regimes and supplies a velocity profile in the region $0 \leq y^+ \leq 70$.

Table 2 presents a comparison of the calculated friction factors with those obtained from empirical correlations available in the literature. The present set of results was obtained on a Pentium 166 MHz microcomputer with a required CPU time of around 11 s.

In the use of the empirical correlation proposed by Webb et al. [14], the roughness function, u_h^+, was represented by Eq. (9b) instead of applying the originally proposed expression in [14], which takes into account the rib pitch only. The overall comparison of the results indicates a good agreement within the range $K_s^+ < 800$. For larger values of the roughness Reynolds number, the computationally predicted results show a progressively increasing discrepancy with respect to those from the two empirical correlations, which still retain a reasonable agreement between them. From these comparisons, especially the ones with regard to the results of the Nikuradse correlation (in [3]), one may conclude that the originally proposed range of applicability for the Cebeci and Bradshaw model [27] to the shift coordinate, represented by $70 < K_s^+ < 2000$, should be exercised with care for values of $K_s^+ > 800$ when employing Eqs. (6c) and (7c).

The range of validity for the correlation proposed by Webb et al. [14] is represented by $0.01 < h_s/D < 0.04$ and $10 < \text{pitch}/h_s < 40$. However, within Table 2, this range was extrapolated up to $\text{pitch}/h_s = 60$ so as to observe its adherence to this extended range and to provide additional comparative observations. It is interesting to note that such results have, nevertheless, a reasonably good agreement with the computationally predicted and the Nikuradse correlation results, the latter valid for $K_s^+ > 70$, and this limitation was obeyed throughout Table 2. This fact sug-

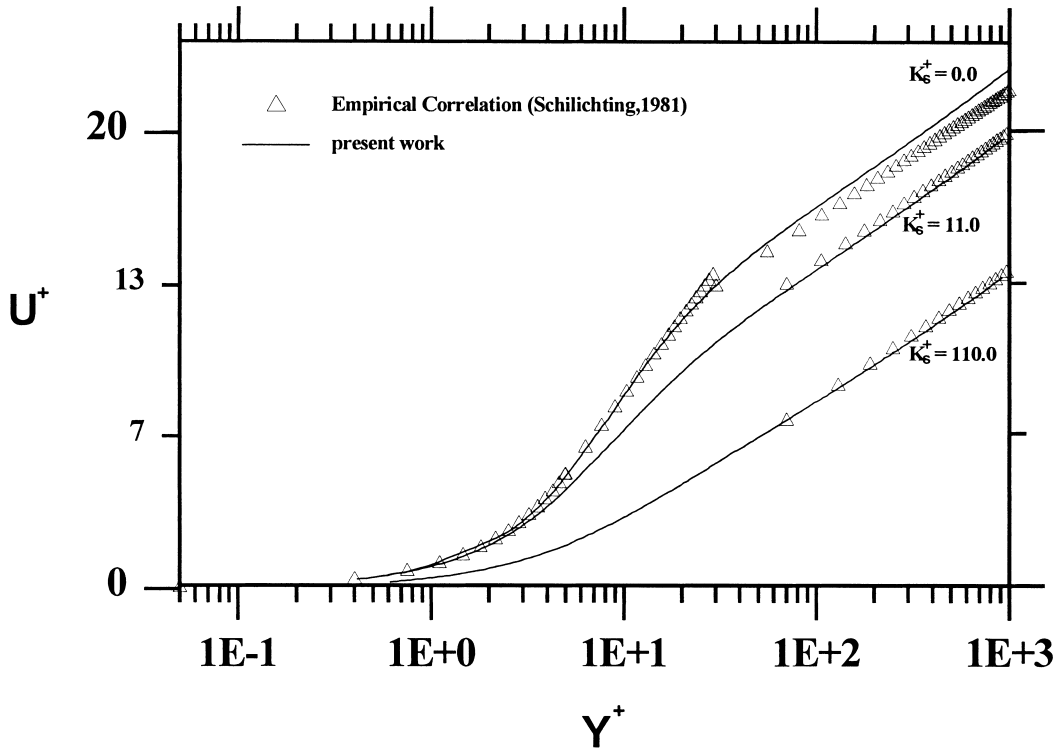

Fig. 1. Comparison of calculated results and empirical correlation for universal velocity profile with different wall roughness factors.

gests that the correlation of Webb et al. [14], when combined with Eq. (9b) proposed by Youn et al. [12] for the roughness friction, might be employed for a slightly extended range than that originally proposed.

4.2. Asymmetric flow

Youn et al. [12] proposed a set of equations to calculate the overall friction factor in rectangular ducts with one side

Table 2
Comparison of friction factors for moderate rib-roughened duct, computational procedure and empirical correlations

h_s/D	Pitch/h	$(K_s/D) \times 10^{-2}$	Webb et al. [14]	This work	Nikuradse [2,3]	K_s^+
			$(f \times 10^2)$	$(f \times 10^2)$	$(f \times 10^2)$	
0.01	20	5.41	1.844	1.846	1.932	519.7
	30	3.61	1.539	1.573	1.606	320.4
	40	2.57	1.337	1.360	1.391	211.9
	50	1.90	1.191	1.188	1.235	146.7
	60	1.45	1.078	1.049	1.117	105.1
0.02	20	11.2	2.710	2.386	2.838	1225.8
	30	7.56	2.190	2.086	2.283	771.6
	40	5.41	1.860	1.847	1.933	520.1
	50	4.03	1.627	1.646	1.687	370.5
	60	3.09	1.453	1.474	1.502	265.6
0.03	20	17.5	3.567	2.748	3.737	2047.0
	30	11.8	2.813	2.429	2.931	1306.5
	40	8.55	2.348	2.178	2.438	892.4
	50	6.41	2.028	1.967	2.100	636.0
	60	4.94	1.792	1.784	1.851	467.0
0.04	20	24.1	4.483	3.037	4.698	2976.5
	30	16.5	3.459	2.701	3.604	1921.4
	40	12.0	2.846	2.440	2.953	1326.4
	50	9.06	2.431	2.221	2.516	955.1
	60	7.02	2.130	2.033	2.200	708.2

Table 3
Overall friction factor at different Reynolds numbers (asymmetric flow)

K_s/D	$Re_D \times 10^{-5}$	Youn et al. [12]	This work	% Difference
		$(f \times 10^2)$	$(f \times 10^2)$	
0.03	0.5	0.9457	0.9257	2.1
	1.0	0.8970	0.8755	2.4
	2.5	0.8468	0.8327	1.6
	5.0	0.8156	0.7444	8.7
0.05	0.5	1.091	1.074	1.6
	1.0	1.040	0.9953	4.3
	2.5	0.9858	0.8951	9.2
	5.0	0.9520	0.8060	15.3

wall rib-roughened, in the form

$$f = \frac{2Hf_1 + W(f_2 + f_3)}{2(W + H)} \tag{13}$$

where W is the channel width, H the height of the rectangular duct and f_1, f_2, and f_3 are the friction factors at the side, bottom and top walls, respectively. The overall friction was validated with a numerical procedure developed by Youn et al. [12] for three different geometries ($H/W = 0.5, 1.0, 2.0$).

In Table 3, results for the overall friction factor (f) are shown by using Eq. (13) in a parallel plate channel $H/W \cong 0$. The friction factors f_2 and f_3 were calculated by the procedure proposed by Youn et al. [12], following the approach presented in this work. As can be seen, the results present deviations for high Reynolds numbers, and this influence may be attributed to the fact that the ratio τ_t/τ_s increases approximately as $U_{max}^{1/5}$ [24] and the flow becomes strongly asymmetric. All of the cases considered here are for $K_s^+ > 70$, thus within the range of validity proposed for Eqs. (9a) and (9b). It should be stressed, though, that Youn's formula Eq. (13) is being extrapolated from the conditions for which it was developed when considering the situation of a parallel plate channel.

A recent work [25] presented experimental results for asymmetric flow in parallel plate channels. The results for the friction velocity

$$u_\tau = \left(u_{\tau 0}^2 + u_{\tau 1}^2\right)^{1/2}$$

normalized by (gSb) and presented in Table 4, confirm that the present procedure can provide important information on pressure drop in practical applications. The position r_m where the shear stress is zero, presents a higher percent difference (8.5%) in the first case due to the higher ratio between the shear stress at the top and the bottom walls. The friction factor results of each wall are also more discrepant in this first case, confirming the influence of the asymmetry level in the flow on the accuracy of the simulation.

5. Conclusions

The analytical procedure presented here has been shown to be appropriate in all the cases analyzed. It is an option of low computational cost in supplying information about the turbulent fully developed velocity profile through smooth, symmetric, and asymmetric moderate rib-roughened channels, very important in the study of turbulent forced convection in ducts with transverse ribs to the flow.

The algebraic turbulence model presented here represents the entire fully developed flow region with good accuracy and shows itself as being an important step in simulating more complex flows, for instance, the turbulent hydrodynamic entrance region in symmetric and asymmetric moderate rib-roughened channels.

The asymmetric flow results are reasonably good for global quantities. The higher deviations in the local friction factor are mainly due to the strongly asymmetric nature of the flow, suggesting that turbulence models which relate Reynolds stress to the velocity gradient cannot simulate such a flow structure adequately. A more detailed discussion on these aspects can be found in [24,28].

In overall terms, from the comparisons with the empirical correlations, the predictive capability of the computational procedure was established in the range of $K_s^+ < 800$.

6. Nomenclature

b	tube radius or distance between plates
D	tube diameter
f	Fanning friction factor, $(2\tau_w/\rho U_0^2)$
H	height of the rectangular duct
K_s/b	relative roughness
K_s^+	sand grain roughness parameter
$L(r)$	dimensionless modified Nikuradse mixing-length

Table 4
Comparison of calculated friction factor, friction velocity and r_m position with experimental results [25]

Re	K_{s_0}/b	K_{s_1}/b	$f_0 \times 10^3$		$f_1 \times 10^3$		$u_\tau/(gSb)^{1/2}$		r_m	
60 800	0.00596	0.0	6.82[a]	6.25[b]	4.69[a]	5.35[b]	0.92[a]	0.93[b]	0.59[a]	0.54[b]
61 000	0.00531	0.0163	7.64	6.76	8.34	7.85	0.90	0.87	0.48	0.46

[a] Experimental data.
[b] Calculated.
g: Gravity acceleration.
$S = 1.97$: Slope of the bed [25].

$\bar{P}$, P	pressure field, dimensional and dimensionless
r_m	position where $\tau = 0$
$\bar{r}$, r	transverse coordinate, dimensional and dimensionless
Re, Re_D	Reynolds number, $U_0 b/\nu$ and $U_0 D/\nu$, respectively
S	slope of the channel or bed
u_{FD}, U_{FD}	fully developed velocity field, dimensional and dimensionless
u_τ	friction velocity
u^+	dimensionless velocity distribution, u_{FD}/u_τ
W	channel width
$\bar{x}$, x	longitudinal coordinate, dimensional and dimensionless
y^+	dimensionless transverse coordinate, ru_τ/ν

Greek Symbols

ν	fluid kinematic viscosity
$\nu_\tau, \varepsilon_{FD}$	turbulent eddy viscosity, dimensional and dimensionless
ρ	fluid density
Δr	shift coordinate
τ	shear stress
τ_w	wall shear stress

Acknowledgements

The authors would like to acknowledge the financial support provided by CAPES, FUJB and CNPq, Brazil, and NSF, USA.

References

[1] J. McEligot, M.D. McEligot, Perspective: some research needs in convective heat transfer for industry, J. Fluids Eng. 116 (1994) 398–404.
[2] J. Nikuradse, Laws for flow in rough pipes, VDI Forschungsheft Series B 361(4) (1950) 1933.
[3] H. Schlichting, Boundary Layer Theory, McGraw-Hill, New York, USA, 1981.
[4] M. Molki, M. Fahri, O. Ozbay, A New correlation for pressure drop in arrays of rectangular blocks in air-cooled electronic units, ASME HTD 237 (1993) 75–81.
[5] J.J. Stukel, P.K. Hopke, K. Nourmohammadi, Turbulent air flow over rough surfaces: mean flow parameters, J. Fluids Eng. 106 (1984) 405–409.
[6] K. Nourmohammadi, P.K. Hopke, J.J. Stukel, Turbulent air flow over rough surfaces II. Turbulent flow parameters, J. Fluids Eng. 107 (1985) 55–60.
[7] H. Yokosawa, H. Fujita, M. Hirota, S. Iwata, Measurement of turbulent flow in a square duct with roughened walls on two opposite sides, Int. J. Heat Fluid Flow 10 (1989) 125–130.
[8] D.F. Dipprey, R.H. Sabersky, Heat and momentum transfer in smooth and rough tubes at various Prandtl numbers, Int. J. Heat Mass Transfer 6 (1963) 329–353.
[9] J.C. Han, Heat transfer and friction in channels with two opposite rib-roughened walls, J. Heat Transfer 106 (1984) 774–781.
[10] K. Ichimiaya, Effects of several roughness elements on an insulated wall for heat transfer from the opposite smooth heated surface in a parallel plate duct, J. Heat Transfer 109 (1987) 68–72.
[11] A.T. Wassel, A.F. Mills, Calculation of variable property turbulent friction and heat transfer in rough pipes, J. Heat Transfer 101 (1979) 469–474.
[12] B. Youn, C. Yuen, A.F. Mills, Friction factor for flow in rectangular ducts with one side rib-roughened, J. Fluids Eng. 116 (1994) 488–493.
[13] R.E. Powe, H.W. Townes, Turbulence structure for fully developed flow in rough pipes, J. Fluids Eng. (1973) 255–261.
[14] R.L. Webb, E.R.G. Eckert, R.J. Goldstein, Heat transfer and friction in tubes with repeated-rib roughness, Int. J. Heat Mass Transfer 14 (1971) 601–617.
[15] Y. Koh, Turbulent flow near a rough wall, J. Fluids Eng. 114 (1992) 537–542.
[16] T.-M. Liou, Y. Chang, D.-W. Hwang, Experimental and computational study of turbulent flows in a channel with two pairs of turbulence promoters in tandem, J. Fluids Eng. 112 (1990) 302–310.
[17] F. Tarada, Prediction of rough-wall boundary layers using a low Reynolds number k-ε model, Int. J. Heat Fluid Flow 11(4) (1990) 331–345.
[18] A.P. Hatton, P.J. Walklate, A mixing-length method for predicting heat transfer in rough pipes, Int. J. Heat Mass Transfer 19 (1976) 1425–1431.
[19] W.J. Feierenisen, M. Acharya, Modeling of transition and surface roughness effects in boundary-layer flows, AIAA J. 24(10) (1986) 1642–1649.
[20] N.L. Vulchanov, V.D. Zimparov, Stabilized turbulent fluid friction and heat transfer in circular tubes with internal sand type roughness at moderate Prandtl numbers, Int. J. Heat Mass Transfer 32(1) (1989) 29–34.
[21] S.L. Han, A mixing length model for turbulent boundary layers over rough surfaces, Int. J. Heat Mass Transfer 34(8) (1991) 2053–2061.
[22] T. Cebeci, K.C. Chang, Calculation of incompressible rough-wall boundary-layer flows, AIAA J. 16(7) (1978) 730–735.
[23] T. Cebeci, K.C. Chang, A general method for calculating momentum and heat transfer in laminar and turbulent duct flows, Num. Heat Transfer 1 (1978) 39–68.
[24] K. Hanjalic, B.E. Launder, Fully developed asymmetric flow in a plane channel, J. Fluid Mech. 51(2) (1972) 301–335.
[25] R.N. Parthasarathy, M. Muste, Velocity measurements in asymmetric turbulent channel flows, J. Hydr. Eng. 120(9) (1994) 1000–1020.
[26] IMSL Library, Math/Lib, Houston, Texas, USA, 1987.
[27] T. Cebeci, P. Bradshaw, Momentum Transfer in Boundary Layers, Hemisphere Publishing Co., Washington DC, USA, 1977.
[28] S. Eskinazi, F.F. Erian, Energy reversal in turbulent flows, Phys. Fluids 12(10) (1969) 1988–1998.